Holographically Printed Freeform Mirror Array for Augmented Reality Near-Eye Display

Jinsoo Jeong, Chang-Kun Lee, Byounghyo Lee, Seungjae Lee, Seokil Moon, Geeyoung Sung, Hong-Seok Lee, and Byoungho Lee, *Fellow, IEEE*

***Abstract*— We propose augmented reality (AR) near-eye display using a holographically printed freeform mirror array. A wide depth of field AR system is implemented by the retinal projection via a small mirror array. Since we use a holographic mirror array, more advantages over a traditional physical mirror array are achieved. Due to the see-through characteristics of the holographic optical element (HOE), the array structure does not obstruct the sight of an observer. Also, the holographic printing technique for the freeform mirror array enables a wide depth of field system without using a floating lens and compensates for the astigmatism of the HOE. The detailed design method of the freeform mirror array HOE is presented. Through the retinal image simulations and the experimental results, the feasibility of the proposed method is verified.**

***Index Terms*— holography, holographic optical components, augmented reality, displays.**

I. Introduction

THE advances in microprocessor, communication, display, and battery technologies have expanded the market of mobile devices. Among them, glasses type augmented reality (AR) devices have received commercial attention due to their hands-free characteristics. In academia, studies on AR devices with compact form factors [1], [2], wide field of view (FOV) [3]–[5], enlarged eye-boxes [6]–[9], and providing focus cue [10], [11] were introduced recently. In the industrial field, not only major companies but startups such as LentinAR [12] and MagicLeap [13] have also recently announced AR glasses technologies and successfully attracted public attention [14].

The desired role of the AR glasses is to provide information of the real scene where the user is looking [15]. In order to respond to a focal change of the user's eyes, AR glasses should change the depth of the displayed image in real-time or provide an image with a wide depth of field (DOF) to see a clear image regardless of the eye focus [16]. To construct the wide DOF AR display, research on retinal projection type near-eye displays (NEDs) has been actively conducted [2]–[4], [8], [17], [18]. The most typical retinal projection type display is a Maxwellian view NED. It projects rays on the retinal plane by focusing them into the center of the eye pupil. Since each ray corresponds one-to-one with a local area on the retina, the Maxwellian view can have a wide DOF and it makes a clear image regardless of the focus of a user [19]. However, the commercialization of the Maxwellian view NED is hindered by the critical drawback: a narrow eye-box. It makes the user difficult to see the displayed image if the pupil of the eye is slightly out of the position where the rays are focused. Several studies have been introduced to extend the eye-box of the Maxwellian view NED by using an eye-tracking method [7], [8], but they need additional devices to steer the eye-box, which makes the glasses heavier.

Manuscript received April 20, 2020; revised June 5, 2020; accepted July 2, 2020. Date of publication July 9, 2020; date of current version July 17, 2020. *(Corresponding author: Byoungho Lee.)*

Jinsoo Jeong, Byounghyo Lee, Seungjae Lee, and Byoungho Lee are with the School of Electrical and Computer Engineering, Seoul National University, Seoul 08826, South Korea (e-mail: dream@snu.ac.kr; yui145263@snu.ac.kr; tmdwo10@snu.ac.kr; byoungho@snu.ac.kr).

Chang-Kun Lee, Seokil Moon, Geeyoung Sung, and Hong-Seok Lee are with the Multimedia Processing Lab, Samsung Advanced Institute of Technology, Samsung Electronics, Suwon 16678, South Korea (e-mail: changkun.lee@samsung.com; seokil.moon@samsung.com; gy.sung@samsung.com; lhs1210@samsung.com).

Color versions of one or more of the figures in this letter are available online at http://ieeexplore.ieee.org.

Digital Object Identifier 10.1109/LPT.2020.3008215

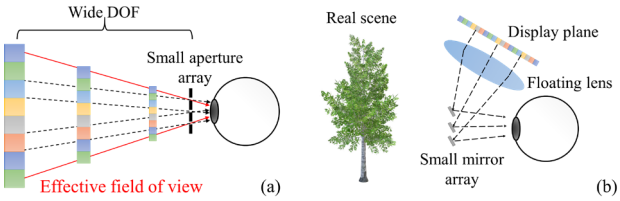

Fig. 1. (a) The basic structure of the small aperture array-based retinal projection display and (b) AR application with small mirror array (LetinAR). The images passing through the small apertures with wide DOF are stitched together in the observer's retinal plane and the observer perceives them as one large image.

II. Previous Work and Proposed Method

A. Previous Work

To overcome the narrow eye-box of the Maxwellian view and provide a wide DOF simultaneously, retinal projection NEDs based on a small aperture array have been introduced by LetinAR and Nvidia [12], [20]. Fig. 1(a) shows the common simplified structure of the display systems. The images with wide DOF displayed by an array of small apertures, such as pinholes or small mirrors, are stitched together in the retinal plane and the observer perceives them as a single large image passing through the large aperture. In this way, the effective FOV of the systems can be enlarged. Besides, due to its array structure, the eye-boxes of the display systems are repeated periodically. However, the structure proposed by Nvidia has a demerit for the AR application since there is a liquid crystal display (LCD) panel between the periodic-pin-structured light sources and the user's eye. The real scene is delivered after it passes through the LCD. It induces a severe diffraction noise and degrades the transparency. In LetinAR's AR glasses,

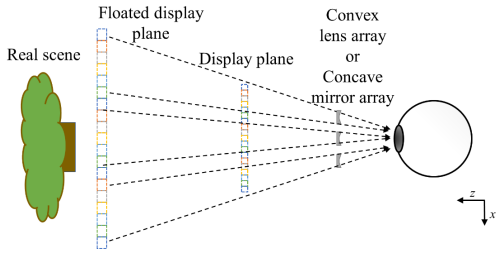

Fig. 2. By replacing the small mirrors with concave mirrors, the display plane can be floated to the desired depth without the floating lens.

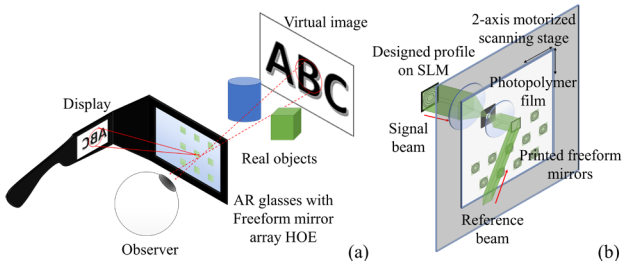

Fig. 3. (a) Concept of the proposed AR NED system using FMA HOE and (b) holographic printing technique to manufacture the HOE. The phase profile of the FMA should be designed by considering the slanted angle of the reference beam and optical aberration, such as astigmatism.

on the other hand, the display is located farther than the small mirror array from the user's eye as shown in Fig. 1(b). As a result, the displayed image and real scene can be merged without diffraction from the pixel structure. The disadvantage of the system is that the physical size of the mirror hinders the sight of the observer and makes the DOF limited. However, as the size of the mirror decreases, there is a trade-off relation by which the amount of light also decreases. To achieve a wide DOF in the desired range with a certain size of a mirror, additional optics (such as a lens) are required to float the display into the virtual space. To make it more compact, the small plane mirrors can be replaced with concave mirrors as shown in Fig. 2. However, the fabrication process of the tiny concave mirrors with a desired curvature inside of the glasses would be too tricky.

B. Proposed Method

The problems can be solved by manufacturing a holographic optical element (HOE) with a holographic printer. Compared to the conventional analog HOE recording method, the holographic printing technique allows fabricating an HOE with a digitally designed function with precise detail [6], [21]. Like a design method of freeform optics [22], it is possible to produce an HOE by calculating the phase distribution. Compared to the traditional freeform optics, HOEs work only at recorded wavelengths and angles, but have very thin thicknesses. Therefore, it is possible to make an AR NED with a smaller form factor. In this Letter, we propose a concept of retinal projection type AR NED using a freeform mirror array (FMA) HOE which is manufactured by a holographic printer. Fig. 3 shows the concept of the proposed method. An FMA HOE is implemented instead of the physical concave mirror array. Since designed freeform mirrors can be recorded instead of the plane mirrors, the display plane can be floated away from the observer's eyes without an additional lens. Also, due to the angular selectivity of the HOE, the FMA

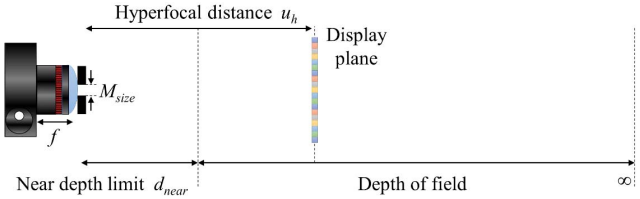

Fig. 4. Concept diagram presenting assumptions for DOF simulation. When the display plane is located on the hyperfocal distance u_h, the DOF of the system is determined as the range from the half of the hyperfocal distance to the infinite plane. If the aperture size M_{size} is 0.8 mm, it satisfies the DOF in the desired depth range (1 m $\sim \infty$).

HOE is transparent to the real scene so that it does not hinder the sight of the observer. Another advantage of the FMA HOE is; it can compensate for the aberrations from the optical system by holographic printing. For example, it is known that astigmatism occurs when using the off-axis HOE lens [23] and we compensate for the error. The FMA HOE can be fabricated using a holographic printer as shown in Fig. 3(b). The reference beam and the signal beam, which is modulated by the spatial light modulator (SLM), are aligned on a photopolymer film and the interference patterns are recorded according to the precise computer-controlled 2-axis motorized linear stage. The freeform mirror with the digitally designed profile can be recorded by displaying the hologram pattern on the SLM. We utilize the holographic printer of [6] with fine-tuning of small details.

III. Design Method of FMA HOE

The important factors in designing an FMA HOE are the size of the mirror M_{size} and the distance between the mirrors D_m, which are determined by the specification of a human eye or a camera. To present the pictures of the experimental results, we designed the FMA HOE according to the camera instead of the eye.

A. The Size of the Mirror

For the first step, we decide the size of the mirror to achieve the DOF in the desired range. We used a smartphone camera that has a 2.52 mm aperture size and a 4 mm distance from the sensor which has a 1.6 μm pixel pitch. We assume a condition that the camera is capturing the display through an aperture, as shown in Fig. 4. For the DOF analysis, we used the concept of the near depth limit and the hyperfocal distance of the camera [24]. When the camera is focusing on the hyperfocal distance, the DOF of the camera can be extended from the near depth limit to the infinite plane. We assume that the camera focuses at a distance range from 1 m to the infinite plane and the display is floated at a distance of 2 m. Based on the assumption, we can determine the aperture size which allows the hyperfocal distance to be 2 m and the near depth limit to be 1 m. The hyperfocal distance u_h and near depth limit d_{near} can be expressed as $u_h = f^2/(Np)$ and $d_{near} = u_h/2$, where f is the focal length of the lens, N is f-number ($N = f/M_{size}$, M_{size} is the size of the aperture) and p is the pixel pitch of the sensor [24]. When deriving the equation, we neglect the distance between the mirror and the camera lens since it is much smaller than the distance from the display plane. Based on the analysis, we decided M_{size} to 0.8 mm to satisfy our assumption.

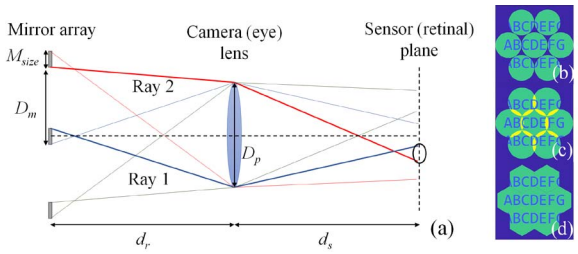

Fig. 5. (a) Conditions to determine the distance D_m between mirrors. d_r is a distance between the mirror array and the pupil, and d_s is a distance between the pupil and the sensor plane. To stitch the images from the mirror array sequentially in the sensor plane, ray 1 and ray 2 must be parallel and matched at the sensor plane. The retinal image simulations when D_m is (b) 3.32 mm, and (c) 2.85 mm without and (d) with pre-image processing.

B. The Distance Between the Mirrors

We designed the distance between the mirrors D_m according to the camera specifications and the determined mirror size M_{size}. For the calculation, we assumed that the angular selectivity of the HOE is enough to cover the whole size of the pupil. Fig. 5(a) shows the condition to be satisfied to tile the images from the mirror array in the sensor plane. To stitch the images sequentially in the sensor plane (in the case of human, retinal plane), ray 1 and ray 2 must be parallel, since the parallel rays are converged to a point in the focal plane of a lens. In general, the ray from the bottom of the mirror k to the top of the lens, and the ray from the top of the adjacent lower mirror $k+1$ to the bottom of the lens (the bold lines) must converge at the sensor plane. The condition can be expressed as $D_m = D_p + M_{size}$, where D_p is a diameter of the camera pupil (lens). In the case of the ideal pinhole, the eye relief d_r does not affect the other parameters. However, in the case of our HOE with 16 μm thickness, the angular selectivity is about $\pm 5°$, and we used the value of d_r as 2 cm. According to the condition, the distance between mirrors D_m can be determined to 3.32 mm, when D_p is 2.52 mm, however, we set the value to 2.85 mm ($\approx 3.32 \times \sqrt{3}/2$) to be filled tightly with hexagonal shapes without vacant space. Figs. 5(b) and 5(c) show the retina image simulations when D_m is 3.32 mm and 2.85 mm with hexagonal shapes. When D_m is 3.32 mm, the circles of the images touch each other in the sensor. However, they cannot be stitched completely. When D_m is 2.85 mm, the tiled image fills the sensor plane without a vacant part of the image, but there are slightly overlapped regions corresponding to the hexagonal shape. We cut the overlapped region out through pre-image processing. Then a continuous clear image is perceived in the sensor as shown in Fig. 5(d).

According to M_{size}, D_m, and the angular selectivity of the HOE θ_{sel}, the eye-box of the system can be defined as Fig. 6. If θ_{sel} is wide enough to cover the pupil when it is shifted by $D_m/2$, as Fig. 6(a), the eye-box can be repeated continuously between the mirrors so it can be extended wide. However, if θ_{sel} is too narrow, the half width of the eye-box is limited by $d_r \cdot \tan\theta_{sel} - (M_{size} + D_p)/2$ as presented in Fig. 6(b).

IV. Experiments and Results

Based on the designed values, we manufactured an FMA HOE using the holographic printer. Table I shows the detailed parameters of the FMA HOE and experimental conditions.

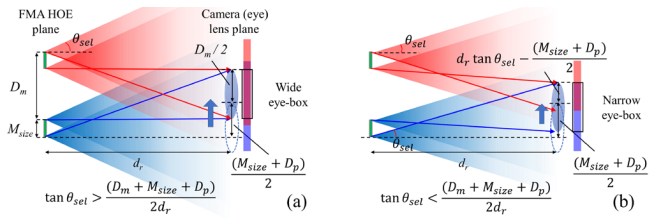

Fig. 6. (a) When the angular selectivity of the HOE θ_{sel} is enough to cover the shifted distance of $D_m/2$, the eye-box can be repeated continuously between the mirrors and become wide. (b) If not, the eye-box is limited narrow by the angular selectivity and discontinuous.

TABLE I
DESIGN AND PRINTING PARAMETERS AND VALUES

Parameter	Value	Parameter	Value
Hyperfocal distance u_h	2 m	Near depth limit d_{near}	1 m
Distance between mirrors D_m	2.85 mm	Mirror size M_{size}	0.8 mm
Minimum focal length in x-direction	24.56 cm	Minimum focal length in y-direction	6.76 cm
Maximum focal length in x-direction	28.60 cm	Maximum focal length in y-direction	8.01 cm
Recording wavelength	532 nm	Number of mirrors	5 × 5
Incidence angle of the reference beam	60°	Incidence angle of the signal beam	0°
Field of view	20°	Average diffraction efficiency	22%
Active size of display plane	3 cm × 2.25 cm	Minimum distance from display plane to HOE	7 cm

An array of 5 × 5 mirrors is recorded with a hexagonal arrangement. The incident angle of the signal beam is 0° and the reference beam is 60° with reflection hologram geometry. We used a 532 nm laser for the coherent light source. The FMA HOE is designed to float the display plane at the hyperfocal distance by assuming the beginning of the x-axis is 7 cm apart from the display plane. In consideration of the change in distance from the display plane due to the off-axis incidence and astigmatism generated by the HOE, the focal lengths in the x and y directions are designed differently in each mirror to prevent the image distortion. The distribution of the designed focal length is presented in Fig. 7(a). For analysis of astigmatism and image distortion by the HOE, we referred to [23]. Fig. 7(a) also shows the manufactured FMA HOE. As presented in Fig. 7(b), the rays from the FMA are tiled without vacant regions when the camera focuses on the hyperfocal distance, which accords with the simulation result. In order to confirm that the fabricated FMA HOE generates the DOF in the desired depth range, we manufacture a plane mirror array HOE in the same way and conduct display experiments to compare. Based on the experimental setup as shown in Fig. 7(c), we captured the image reflected from the mirror array HOE and the FMA HOE with the camera's focal plane varying from 10 cm to 3 m. As shown in Fig. 7(d), the plane mirror array HOE generates the DOF in the near distance, but the FMA HOE produces a clearer image in the far distance as we designed. By the experimental results, we verify that the display plane can be floated in the desired depth range without any additional optical element. For the display, we use a green LED projector and a diffuser screen. At this time, we implemented the display with a projection display system,

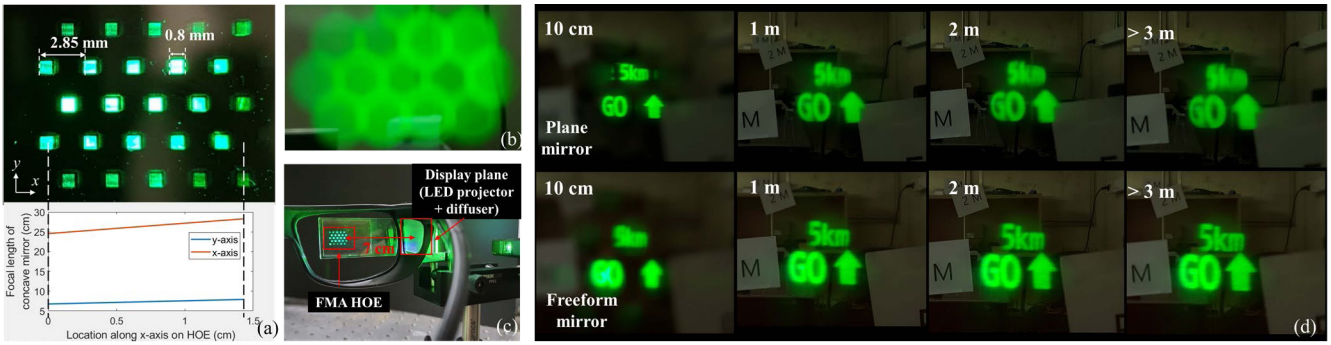

Fig. 7. (a) The manufactured result of the FMA HOE with a profile of the focal length. (b) When the camera focuses far enough, the images from the array are stitched compact in the camera sensor plane. (c) The experimental setup of the display system. (d) The experimental results of comparing DOF. The focal plane of the camera is varying from 10 cm to 3 m. The HOE with plane mirror array has DOF range near the HOE plane and HOE with FMA has DOF range far from the HOE plane.

but if we later replace it with a microdisplay panel (micro-LED/OLED/LCoS), the setup can be more straightforward and compact. Also, the diffraction efficiency can be improved by reducing the vibration of the holographic printer and flickering from the SLM.

The above experiment shows that the design method works well for the camera and all the principles that we used can be applied to human eyes. This means that the same design method works for a measured pupil size of a human eye.

V. Conclusion

We proposed a design and fabrication method of an AR NED system using FMA HOE as an image combiner. The FMA HOE was designed digitally and manufactured by a holographic printing technique. The system has an extended eye-box based on its periodic structure and has wide DOF based on the small aperture size. The advantage of the method is that the freeform profile of each mirror can be printed precisely and it can float the display plane in desired depth without any additional optical element. For the future work, we will manufacture the light-guide type FMA HOE, and optimize the direction of the reference beam and the aperture shape to enhance the quality, such as brightness and form factor.

Acknowledgment

Covestro AG provided the photopolymer Bayfol HX film used in experiment.

References

[1] Q. Gao, J. Liu, X. Duan, T. Zhao, X. Li, and P. Liu, "Compact see-through 3D head-mounted display based on wavefront modulation with holographic grating filter," *Opt. Express*, vol. 25, no. 7, pp. 8412–8424, Apr. 2017.

[2] A. Maimone, A. Georgiou, and J. S. Kollin, "Holographic near-eye displays for virtual and augmented reality," *ACM Trans. Graph.*, vol. 36, no. 4, Jul. 2017, Art. no. 85.

[3] C. Jang, K. Bang, S. Moon, J. Kim, S. Lee, and B. Lee, "Retinal 3D: Augmented reality near-eye display via pupil-tracked light field projection on retina," *ACM Trans. Graph.*, vol. 36, no. 6, Nov. 2017, Art. no. 190.

[4] S. Moon *et al.*, "Augmented reality near-eye display using pancharatnam-berry phase lenses," *Sci. Rep.*, vol. 9, Apr. 2019, Art. no. 6616.

[5] G.-Y. Lee *et al.*, "Metasurface eyepiece for augmented reality," *Nature Commun.*, vol. 9, Nov. 2018, Art. no. 4562.

[6] J. Jeong, J. Lee, C. Yoo, S. Moon, B. Lee, and B. Lee, "Holographically customized optical combiner for eye-box extended near-eye display," *Opt. Express*, vol. 27, no. 26, pp. 38006–38018, Dec. 2019.

[7] J. Kim *et al.*, "Foveated AR: Dynamically-foveated augmented reality display," *ACM Trans. Graph.*, vol. 38, no. 4, Jul. 2019, Art. no. 99.

[8] C. Yoo, M. Chae, S. Moon, and B. Lee, "Retinal projection type lightguide-based near-eye display with switchable viewpoints," *Opt. Express*, vol. 28, no. 3, pp. 3116–3135, Feb. 2020.

[9] J.-H. Park and S.-B. Kim, "Optical see-through holographic near-eye-display with eyebox steering and depth of field control," *Opt. Express*, vol. 26, no. 21, pp. 27076–27088, Oct. 2018.

[10] S. Lee, Y. Jo, D. Yoo, J. Cho, D. Lee, and B. Lee, "Tomographic near-eye displays," *Nature Commun.*, vol. 10, Jun. 2019, Art. no. 2497.

[11] X. Hu and H. Hua, "High-resolution optical see-through multi-focal-plane head-mounted display using freeform optics," *Opt. Express*, vol. 22, no. 11, pp. 13896–13903, Jun. 2014.

[12] LetinAR. *Innovate Pin Mirror Technology*. Accessed: Apr. 1, 2020. [Online]. Available: https://letinar.com/technology

[13] M. L. Corporation. *Magic Leap 1*. Accessed: Apr. 1, 2020. [Online]. Available: https://www.magicleap.com/magic-leap-1

[14] B. C. Kress, "Optical waveguide combiners for AR headsets: Features and limitations," *Proc. SPIE*, vol. 11062, Jul. 2019, Art. no. 110620J.

[15] J. Carmigniani, B. Furht, M. Anisetti, P. Ceravolo, E. Damiani, and M. Ivkovic, "Augmented reality technologies, systems and applications," *Multimedia Tools Appl.*, vol. 51, pp. 341–377, Dec. 2010.

[16] K. Rathinavel, H. Wang, A. Blate, and H. Fuchs, "An extended depth-at-field volumetric near-eye augmented reality display," *IEEE Trans. Vis. Comput. Graph.*, vol. 24, no. 11, pp. 2857–2866, Nov. 2018.

[17] Y. Wu *et al.*, "Design of retinal-projection-based near-eye display with contact lens," *Opt. Express*, vol. 26, no. 9, pp. 11553–11567, Apr. 2018.

[18] C. P. Chen *et al.*, "Design of retinal projection displays enabling vision correction," *Opt. Express*, vol. 25, no. 23, pp. 28223–28235, Oct. 2017.

[19] Y. Takaki and N. Fujimoto, "Flexible retinal image formation by holographic Maxwellian-view display," *Opt. Express*, vol. 26, no. 18, pp. 22985–22999, Sep. 2018.

[20] A. Maimone, D. Lanman, K. Rathinavel, K. Keller, D. Luebke, and H. Fuchs, "Pinlight displays: wide field of view augmented reality eyeglasses using defocused point light sources," *ACM Trans. Graph.*, vol. 33, no. 4, Jul. 2014, Art. no. 89.

[21] K. Wakunami *et al.*, "Projection-type see-through holographic three-dimensional display," *Nature Commun.*, vol. 7, Oct. 2016, Art. no. 12954.

[22] D. Cheng, Y. Wang, H. Hua, and M. M. Talha, "Design of an optical see-through head-mounted display with a low f-number and large field of view using a freeform prism," *Appl. Opt.*, vol. 48, no. 14, pp. 2655–2668, May 2009.

[23] S. Lee, B. Lee, J. Cho, C. Jang, J. Kim, and B. Lee, "Analysis and implementation of hologram lenses for see-through head-mounted display," *IEEE Photon. Technol. Lett.*, vol. 29, no. 1, pp. 82–85, Jan. 1, 2017.

[24] J. E. Greivenkamp, *Field Guide to Geometrical Optics*. Bellingham, WA, USA: SPIE Press, 2004.